Adaptive Codebook-Based Channel Estimation in OFDM-Aided Hybrid Beamforming mmWave Systems

YAOYUAN ZHANG, MOHAMMED EL-HAJJAR (Senior Member, IEEE), AND LIE-LIANG YANG (Fellow, IEEE)

School of Electronics and Computer Science, University of Southampton, SO17 1BJ Southampton, U.K.

CORRESPONDING AUTHOR: M. EL-HAJJAR (e-mail: meh@ecs.soton.ac.uk)

ABSTRACT In order to reduce the hardware complexity and cost of mmWave transceivers, hybrid beamforming techniques have been developed, which rely on the channel state information (CSI) available to the receiver and/or transmitter. In mmWave channel estimation, the compressed sensing (CS)-based algorithms like orthogonal matching pursuit (OMP) have been widely studied to take the advantages of the sparse characteristics of mmWave channels. Specifically, the OMP-assisted adaptive codebook channel estimation has the merit of reduced implementation complexity, but it performs undesirably in low signal to noise ratio (SNR) scenarios. To circumvent this problem, in this paper, we develop an improved adaptive codebook channel estimation algorithm for orthogonal frequency division multiplexing (OFDM) mmWave systems, which enhances the estimation performance by exploiting the multi-carrier signals for joint decision making. Our studies show that the proposed channel estimation is capable of significantly improving the estimation accuracy at low SNR, while enjoying a low complexity for implementation.

INDEX TERMS mmWave, channel estimation, adaptive codebook, OFDM, hybrid beamforming.

I. INTRODUCTION

GIVEN the rapid increase of the number of connected devices, new spectrums have to be discovered to meet the near-future demand on wireless communications [1]. According to prediction, wireless data traffic is expected to increase more than $10,000$ folds in the next decades [2]. One potential solution to solve the bandwidth shortage problem is to exploit the millimeter wave (mmWave) band [1]. However, mmWave signals suffer from significant pathloss [3]. Meanwhile, there are many other factors affecting the quality of mmWave transmissions, which include atmospheric attenuation, rain fading and material penetration [1], [3]. Therefore, in mmWave communications, the antenna arrays with high-efficiency and low-complexity beamforming are required for enhancing the transmission quality. On the bright side, owing to the short wavelength of mmWave signals, a large number of antennas may be fitted in a relatively small space, which allows to employ the massive multiple-input multiple output (MIMO) techniques to enhance the performance of communications [1].

As demonstrated in literature, mmWave massive MIMO is capable of providing a high beamforming gain to attain a high spectral efficiency (SE), which hence can compensate for the high pathloss in mmWave communications [4]. Traditionally, beamforming can be implemented using either digital or analog signal processing techniques. While the digital beamforming can control both the phase and amplitude of the transmitted/received signals, it however requires a distinct radio frequency (RF) chain per antenna element [5], [6], [7], [8]. This implementation results in dramatic power consumption and hardware cost, in particular, when a large antenna array is employed. By contrast, the analog beamforming only uses analog phase shifters to control the phases of the transmitted/received signals. It requires only a single RF chain, which can significantly reduce the implementation complexity and power consumption [9]. However, the performance of analog beamforming is usually worse than that of digital beamforming, as the result of the constant amplitude constraint on the analog phase shifters and the relatively poor control of signals' phases. Furthermore, the performance of analog beamforming may be further degraded in multi-user systems, due to its weaker interference management capability in comparison with the digital beamforming. Therefore, in mmWave

communications, hybrid beamforming has been developed and intensively studied, so as to attain the performance of digital beamforming in multi-user scenarios, while at the reduced cost and power consumption [10], [11], [12].

Similar to the other wireless systems, the achievable rate of a mmWave system is constrained by the accuracy of the estimated channel state information (CSI) [1], [13], [14], which can also significantly affect the performance of the beamforming, no matter whether it implements analog, digital or hybrid beamforming [15]. From the studies and practical measurements, we know that the channel models for microwave bands are very different from the mmWave channel models, where sparse scattering exists, causing a big time dispersion [16]. In other words, mmWave channels are typically sparse channels, as the result of limited environmental scattering and the high space-time resolution of mmWave signals [4]. For this sake, the traditional linear channel estimators, such as least square (LS), are not efficient for the mmWave channel estimation. This is because a high pilot overhead is usually required, when a sparse channel is estimated by the conventional linear estimators [4]. Therefore, in mmWave massive MIMO systems, many channel estimation algorithms are based on the principle of compressed sensing (CS) [17], [18], [19], as it can efficiently solve the sparse channel estimation problem, and enables to achieve promising system performance [15], [20]. For example, in [13], a closed-loop sparse channel estimation method was proposed for the wideband mmWave full-dimensional MIMO systems. By simultaneously considering both the angle and delay domains, the proposed algorithm is capable of achieving the channel estimation of high-accuracy. Furthermore, in [20], a CS-relied Beam Split Pattern Detection (BSPD)-based channel estimation scheme was proposed for the channel estimation in the Terahertz (THz) massive MIMO systems.

In the context of CS, the orthogonal matching pursuit (OMP) algorithm is one of the popular algorithms applied for different purposes in wireless communications [21]. To be more specific, the authors of [22] proposed an OMP-based open-loop channel estimation algorithm for the mmWave MIMO systems with hybrid beamforming. In this study, the channel model was assumed to be an angle-grid channel, representing a parametric channel with the quantized angle-of-departure (AoD) and angle-of-arrival (AoA). In [14], the authors proposed two OMP-based compressed channel estimation algorithms for orthogonal frequency division multiplexing (OFDM) systems, which make use of the joint sparse recovery to estimate the channel information shared by different subcarriers. In [17], an adaptive codebook-based channel estimator was developed, where CSI is inferred by the designed codebook that also provides the beamforming vectors for training. In [17], the OMP-based method was used for both channel estimation and codebook design. The study shows that the proposed method outperforms the traditional OMP-based channel estimation, while also enjoying a lower complexity. In [23], the authors proposed a so-called iterative reweight (IR)-based super-resolution channel

estimation algorithm for the mmWave MIMO systems with hybrid beamforming. It was shown that this channel estimation algorithm is capable of achieving an improved mean square error (MSE) performance, when compared with the adaptive codebook-based and the traditional OMP-based channel estimation techniques. Furthermore, a singular value decomposition (SVD)-based precoding method was presented in [23], so as to overcome the high computational burden of the IR-based channel estimation. However, the adaptive codebook-based channel estimation suffers from the poor performance in low SNR region, which is a common disadvantage in the OMP-based channel estimation. To mitigate this problem, in this paper, we propose a multi-carrier joint decision making scheme to enhance the performance of the adaptive codebook-based channel estimation.

Our motivation lies in the fact that OFDM and its variants have now been commonly used in the various wireless systems for combating channel fading, interference and multi-path effects [24]. Therefore, it is beneficial to exploit the multi-carrier signals for improving the performance of channel estimation in the OFDM-relied mmWave systems. In summary, the novel contributions in this paper can be stated as follows:

- A channel estimation scheme for the mmWave OFDM systems with hybrid beamforming is proposed, which uses an adaptive codebook to estimate the AoD/AOA by jointly exploiting the signals conveyed by different subcarriers, so as to improve the overall accuracy of channel estimation.

- A multi-carrier joint decision making scheme is proposed to enhance the performance of the adaptive codebook-based channel estimation. With this scheme, the channel estimated from different subcarriers at a stage are jointly exploited to select an angle range with improved accuracy for supporting the next stage of channel estimation, which hence enhances the overall estimation accuracy in comparison with the conventional adaptive codebook assisted channel estimation.

- The simulation results show that the MSE achieved by the proposed channel estimation scheme can be 8 times lower than that obtained by the conventional codebook-based counterpart. Additionally, the spectral efficiency (SE) attained by a mmWave OFDM system with the proposed channel estimation is nearly identical to that attained by the corresponding mmWave OFDM system assuming perfect CSI, which is about 3 bits/sec/Hz higher than that attained by the mmWave OFDM system with the conventional codebook-based counterpart.

The rest of this paper is organized as follows: the system model and the mmWave channel model are presented in Section II. In Section III, both the traditional adaptive codebook-based channel estimation and the proposed channel estimation are described. Section IV presents and discusses the simulation results. Finally, our conclusions are summarized in Section V.
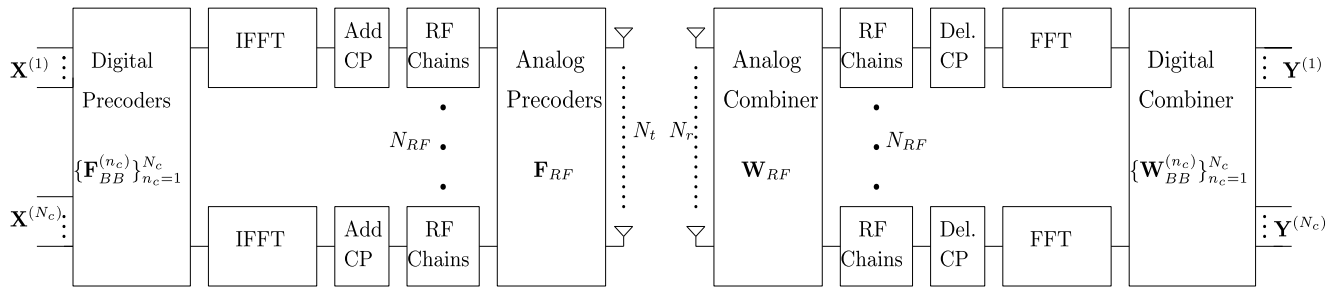
FIGURE 1. Block diagram of mmWave OFDM system.

The notations used in this paper are as follows: Lower-case and upper-case boldface letters $\boldsymbol{a}$ and $\boldsymbol{A}$ denote vectors and matrices, respectively; $(\cdot)^T$ and $(\cdot)^H$ express the transpose and conjugate transpose, respectively; $\mathbb{C}^{M \times N}$ is the set of $(M \times N)$-element in the complex field; $\mathbb{E}[\cdot]$ is the expectation operator; $\otimes$ is the matrix Kronecker product; $\text{Mode}(\boldsymbol{a})$ is the mode of the elements in vector $\boldsymbol{a}$; $\lceil \cdot \rceil$ is the ceiling operator; $\| \cdot \|_F$ is the Frobenius norm; $vec\{\cdot\}$ denotes vectorization.

II. SYSTEM MODEL

In this section, we first present the mmWave OFDM system with hybrid beamforming, whose block diagram is shown in Fig. 1. Then, we elaborate on the mmWave channel model employed in our study in both the frequency domain and the beamspace domain.

A. MODELING OF MMWAVE OFDM SYSTEM WITH HYBRID BEAMFORMING

Consider a mmWave OFDM system with N_t transmit antennas and N_r receive antennas, as shown in Fig. 1, where N_c denotes the number of subcarriers. Let $\boldsymbol{x}^{(n_c)} \in \mathbb{C}^{N_s \times 1}$ and $\boldsymbol{y}^{(n_c)} \in \mathbb{C}^{N_s \times 1}$ denote the transmitted symbol vector and received symbol vector, respectively, with respect to the n_c-th subcarrier, where N_s denotes the number of data streams transmitted in parallel on one subcarrier. Let $\boldsymbol{F}_{BB}^{(n_c)}$ and $\boldsymbol{W}_{BB}^{(n_c)}$ denote the baseband precoder and combiner, respectively, for the n_c-th subcarrier. Furthermore, we assume that there are $N_{RF}^{(t)}$ RF chains at transmitter and $N_{RF}^{(r)}$ RF chains at receiver. We assume that the number of RF chains is significantly smaller than the corresponding number of antennas, i.e., $N_{RF}^{(t)} \ll N_t$, and $N_{RF}^{(r)} \ll N_r$. Additionally, the mmWave channel matrix is denoted as $\boldsymbol{H} \in \mathbb{C}^{N_r \times N_t}$. Then, it can be shown that the received signals from the n_c-th subcarrier of the N_r receive antennas can be expressed as

$$\boldsymbol{y}^{(n_c)} = \left(\boldsymbol{W}^{(n_c)}\right)^H \boldsymbol{H}^{(n_c)} \boldsymbol{F}^{(n_c)} \boldsymbol{x}^{(n_c)} + \left(\boldsymbol{W}^{(n_c)}\right)^H \boldsymbol{n}^{(n_c)}, \quad (1)$$

where

$$\boldsymbol{F}^{(n_c)} = \boldsymbol{F}_{RF} \boldsymbol{F}_{BB}^{(n_c)}, \quad (2)$$

$$\boldsymbol{W}^{(n_c)} = \boldsymbol{W}_{RF} \boldsymbol{W}_{BB}^{(n_c)}. \quad (3)$$

As shown in (1)-(3), the data symbols $\boldsymbol{x}^{(n_c)}$ are first processed by the digital precoder $\boldsymbol{F}_{BB}^{(n_c)} \in \mathbb{C}^{N_{RF}^{(t)} \times N_s}$ for

$n_c = 1, 2, \ldots, N_c$. Then, the N_c outputs corresponding to the same transmit antenna are collected to form a vector, which is sent to the inverse fast Fourier Transform (IFFT) to transform to the time domain. Then, the cyclic prefix (CP) is added, followed by the analog precoding processing by $\boldsymbol{F}_{RF} \in \mathbb{C}^{N_t \times N_{RF}^{(t)}}$ for all the N_t transmit antennas before it is transmitted. In (1), $\boldsymbol{n}^{(n_c)} \in \mathbb{C}^{N_r \times 1}$ denotes a complex independent identically distributed (i.i.d.) Gaussian noise vector, which is distributed with zero-mean and a covariance matrix $\sigma^2 \boldsymbol{I}$, where σ^2 denotes the noise power.

At the receiver side, an analog combiner $\boldsymbol{W}_{RF}$ is first used for combining the received signal in the analog domain. Then, the CP is removed followed by an N_c-point FFT to transform signals to frequency domain. Then, the N_t outputs belonging to the same subcarriers are collected to form a vector. Finally, for Subcarrier $n_c = 1, 2, \ldots, N_c$, a baseband digital combiner $\boldsymbol{W}_{BB}^{(n_c)}$ is applied to obtain $\boldsymbol{y}^{(n_c)}$, as shown in (1). Considering all the N_c subcarriers, we form a vector $\boldsymbol{y} = [(\boldsymbol{y}^{(1)})^T, (\boldsymbol{y}^{(2)})^T, \ldots, (\boldsymbol{y}^{(N_c)})^T]^T$.

From above we can know that both the precoding and combining are dependent on the channel. Hence, in order to recover the transmitted symbol vector $\boldsymbol{x}$, it is essential to have the channel state information (CSI) of high-accuracy, which can be acquired using the channel estimation to be addressed in Section III.

B. CHANNEL MODEL

Given a uniform linear array (ULA),[1] the mmWave channel model with L scatters is assumed. We assume that each scatter generates one path from transmitter to receiver. Hence the channel matrix can be represented as [17],

$$\boldsymbol{H}^{(n_c)} = \sqrt{\frac{N_t N_r}{L}} \sum_{l=1}^{L} \alpha_l^{(n_c)} \boldsymbol{a}_r(\phi_l) \boldsymbol{a}_t^H(\theta_l), \ n_c = 1, 2, \ldots, N_c, \quad (4)$$

where $\alpha_l^{(n_c)}$ is the complex gain of the l-th path. θ_l and ϕ_l are the azimuth AoD and AoA, respectively. Since the ULA array is considered, the response vector $\boldsymbol{a}_{ULA}$ for a given

---

1. ULA is used mainly for simplicity, but the design and analysis in this paper apply to any types of antenna structures.

AoD or AoA of ϕ can be expressed as [25]

$$\boldsymbol{a}_{ULA}(\phi) = \frac{1}{\sqrt{N_x}} \left[1, e^{j\frac{2\pi}{\lambda}\sin(\phi)}, \ldots, e^{j(N_x-1)\frac{2\pi}{\lambda}\sin(\phi)} \right]^T, \quad (5)$$

where N_x is either N_t or N_r, λ is the wavelength, and d denotes the inter-element spacing of the ULA.

As mentioned previously, CSI is required for the design of beamformers, both the knowledge about the AoDs and AoAs as well as that about the channel gains are required [4]. Considering the sparse characteristics of mmWave channels, the CS relied methods are suitable for solving the mmWave channel estimation problem [1], where the size of the dictionary for CS is significantly larger than the size of the measurement vector [4]. Specifically in the problem of mmWave channel estimation, the size of the dictionary is dependent on the size of AoAs and AoDs, while the size of the measurement vector depends on the number of the ULA elements.

Let us divide the possible AoD and AoA with the range of $[0, \pi)$ equally into $G_T \geq max\{N_t, N_r\}$ and $G_R \geq max\{N_t, N_r\}$ angles by utilizing the angle space partition method introduced in [22]. Then, the quantized AoDs and quantized AoAs should satisfy the relationships of [22]

$$\cos\left(\theta_g^{(t)}\right) = \frac{2(g-1)}{G_T} - 1, \quad 1 \leq g \leq G_T, \quad (6)$$

$$\cos\left(\phi_g^{(r)}\right) = \frac{2(g-1)}{G_R} - 1, \quad 1 \leq g \leq G_R. \quad (7)$$

Let us collect the quantized AoDs and AoAs to form the sets of $\boldsymbol{\Theta}$ and $\boldsymbol{\Phi}$, which are denoted as [22]

$$\boldsymbol{\Theta} = \left\{ \theta_g^{(t)} : \theta_g^{(t)} \in [0, \pi), 1 \leq g \leq G_T \right\}, \quad (8)$$

$$\boldsymbol{\Phi} = \left\{ \phi_g^{(r)} : \phi_g^{(r)} \in [0, \pi), 1 \leq g \leq G_R \right\}. \quad (9)$$

Based on $\boldsymbol{\Theta}$ and $\boldsymbol{\Phi}$, now the transmit and receive array response dictionary matrices can be written as

$$\boldsymbol{A}_T(\boldsymbol{\Theta}) = \left[\boldsymbol{a}_t\left(\theta_1^{(t)}\right), \boldsymbol{a}_t\left(\theta_2^{(t)}\right), \ldots, \boldsymbol{a}_t\left(\theta_{G_T}^{(t)}\right) \right], \quad (10)$$

$$\boldsymbol{A}_R(\boldsymbol{\Phi}) = \left[\boldsymbol{a}_r\left(\phi_1^{(r)}\right), \boldsymbol{a}_r\left(\phi_2^{(r)}\right), \ldots, \boldsymbol{a}_r\left(\phi_{G_R}^{(r)}\right) \right], \quad (11)$$

which satisfy [22]

$$\boldsymbol{A}_T(\boldsymbol{\Theta})(\boldsymbol{A}_T(\boldsymbol{\Theta}))^H = \frac{G_T}{N_t}\boldsymbol{I}_{N_t}, \quad (12)$$

$$\boldsymbol{A}_R(\boldsymbol{\Phi})(\boldsymbol{A}_R(\boldsymbol{\Phi}))^H = \frac{G_R}{N_r}\boldsymbol{I}_{N_r}, \quad (13)$$

which, except the constant factors, are Hermition matrices. As explained in [22], $\boldsymbol{A}_T(\boldsymbol{\Theta})$ determines a transmit beamspace, while $\boldsymbol{A}_R(\boldsymbol{\Phi})$ determines a receive beamspace. Consequently, the frequency domain channel $\boldsymbol{H}^{(n_c)}$ can be represented with the aid of a beamspace channel $\boldsymbol{H}_b^{(n_c)}$ as

$$\boldsymbol{H}^{(n_c)} = \boldsymbol{A}_R \boldsymbol{H}_b^{(n_c)} \boldsymbol{A}_T^H, \quad (14)$$

where $\boldsymbol{\Theta}$ in $\boldsymbol{A}_T(\boldsymbol{\Theta})$ and $\boldsymbol{\Phi}$ in $\boldsymbol{A}_R(\boldsymbol{\Phi})$ are ignored for the sake of simplicity of presentation. Note that $\boldsymbol{H}_b^{(n_c)}$ is a $(G_R \times G_T)$-dimensional matrix, with the (u, v)-th element

being the channel gain at the AoD of $\theta_v^{(t)}$ and the AoA of $\phi_u^{(r)}$. From (4) we know that there are only L paths from transmitter to receiver. This means that in the ideal case that all practical AoDs/AOAs align perfectly with the quantized AoDs/AoAs grids, $\boldsymbol{H}_b^{(n_c)}$ is a sparse matrix having only L nonzero elements. In practice, the quantized AoDs/AoAs cannot fully match with the actual AoDs/AoAs and furthermore, the quantized AoDs/AOAs are not necessary orthogonal. Consequently, the number of nonzero elements in $\boldsymbol{H}_b^{(n_c)}$ is in general more than L.

For convenience of channel estimation, let us vectorize (14) to obtain

$$\boldsymbol{h}^{(n_c)} = \left(\boldsymbol{A}_T^* \otimes \boldsymbol{A}_R\right)\boldsymbol{h}_b^{(n_c)}, \quad (15)$$

where $\boldsymbol{h}_b^{(n_c)} = vec\{\boldsymbol{H}_b^{(h_c)}\}$. In the beam-space based channel estimation, the AoDs/AoAs can be first found via identifying the locations of the nonzero elements in $\boldsymbol{h}_b^{(n_c)}$. Then, the corresponding channels gains, given by the values of the nonzero elements in $\boldsymbol{h}_b^{(n_c)}$, can be estimated. Let us now detail the codebook-based channel estimation.

III. ADAPTIVE CODEBOOK-BASED CHANNEL ESTIMATION

In this section, first, the conventional adaptive codebook-based channel estimation [17] is introduced. Then, this approach is extended to the OFDM systems, where channel estimation is enhanced with the aid of the multiple carrier joint decision making.

A. CONVENTIONAL ADAPTIVE CODEBOOK-BASED CHANNEL ESTIMATION

The codebook-based techniques can be employed for both precoder and combiner design. With the codebook-based techniques, after the channel state information (CSI) is obtained, the transmitter and receiver respectively select the most appropriate entries from the codebook as the precoder and combiner, rather than directly designing the precoder and combiner using the optimization algorithms [26], [27]. For example, the OMP-based channel estimation can be improved for designing the precoder and combiner based on the pre-designed codebook, which results in an improved accuracy of estimation, as shown in [11].

Our approach represents the extension of the adaptive codebook-based channel estimation algorithm proposed in [17]. Based on this algorithm, the range of AoD (AoA) is firstly divided into K^{s-1} subsets at the s-th stage, $s = 1, 2, \ldots, S$, with each subset containing K beamforming codewords, where S is the number of stages and $K \geq 2$ is a constant. The $K \times K^{s-1}$ codewords at the s-th stage form a set $\mathcal{F}_s$, and the m-th codeword in subset k at the s-th stage is expressed as $[\boldsymbol{F}_{(s,k)}]_{:,m}$, which is a vector of length N_t (or N_r), when transmitter (or receiver) codebook is considered. The structure of the codebook can be readily understood by referring to the example as shown in Fig. 2, where $S = 3$ and $K = 2$ are assumed. Hence, the 1-st stage has one
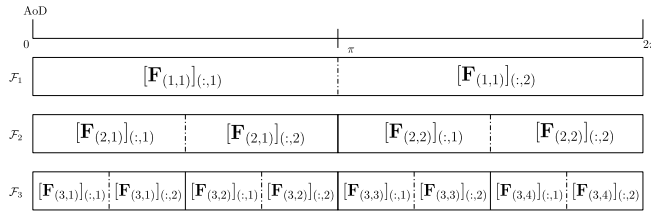
FIGURE 2. Multi-resolution codebook structure with $S = 3$ stages and each subset having $K = 2$ codewords.

subset containing 2 codewords, 2-nd stage has 2 subsets of each containing 2 codewords, and 3-rd stage has 4 subsets of each containing 2 codewords. The total number of codewords is 14. Fig. 2 also shows the corresponding angle range associated with a codeword. Specifically for $s = 2$, the angle ranges associated with the 4 codewords are $[0, \frac{\pi}{2})$, $[\frac{\pi}{2}, \pi)$, $[\pi, \frac{3\pi}{2})$, and $[\frac{3\pi}{2}), 2\pi)$, respectively.

According to [17], the codebook for the precoder (the same for the combiner) at the s-th stage can be designed as

$$\boldsymbol{a}_t^H(\phi_u)\big[\boldsymbol{F}_{(s,k)}\big]_{(:,m)} = \begin{cases} C_s, & \text{if} \quad u \in \mathcal{I}_{(s,k,m)}, \\ 0, & \text{otherwise}, \end{cases} \quad (16)$$

where $\mathcal{I}_{(s,k,m)} = \{\frac{N}{K^s}(K(k-1)+m-1)+1, \ldots, \frac{N}{K^s}(K(k-1)+m)\}$ defines the sub-range of AoDs associated with the codeword $[\boldsymbol{F}_{(s,k)}]_{(:,m)}$, $N = G_T$ (or G_R), and C_s is a normalization constant. Equation (16) explains that the cross-correlation between the array response vector $\boldsymbol{a}_t(\phi_u)$ and $[\boldsymbol{F}_{(s,k)}]_{(:,m)}$ is C_s, provided that the AoD ϕ_u falls in the sub-range managed by $[\boldsymbol{F}_{(s,k)}]_{(:,m)}$. Otherwise, if ϕ_u is not in the sub-range controlled by $[\boldsymbol{F}_{(s,k)}]_{(:,m)}$, the above cross-correlation is zero, meaning orthogonal.

Using this method, a best possible precoder (or combiner) for a given angle can be obtained after a few stages of search, so that the array can transmit to (or receive from) the beam in the specific direction.

When considering all the possible beam angles, from (16), a generalized formula for the precoder $\boldsymbol{F}_{(s,k)}$ of the s-th stage and k-th subset can be obtained by solving the equation

$$\boldsymbol{A}_T^H \boldsymbol{F}_{(s,k)} = C_s \boldsymbol{G}_{(s,k)}, \quad (17)$$

where $\boldsymbol{G}_{(s,k)}$ is a $(G_T \times K)$ matrix, which consists of the elements of 1s and 0s. Specifically, the elements in the m-th column of $\boldsymbol{G}_{(s,k)}$ are equal to 1, if $m \in \mathcal{I}_{s,k,m}$. Otherwise, they are equal to 0. From (17), we can readily know that one approximate solution is given by [17]

$$\boldsymbol{F}_{(s,k)} = C_s \big(\boldsymbol{A}_T \boldsymbol{A}_T^H\big)^{-1} \boldsymbol{A}_T \boldsymbol{G}_{(s,k)}. \quad (18)$$

Let $\boldsymbol{X} = [\boldsymbol{x}_1, \boldsymbol{x}_2, \ldots, \boldsymbol{x}_{N_s}]$ denote the measurement training matrix, which is formed by the pilot data expressed as $\boldsymbol{X} = \sqrt{P}\boldsymbol{I}_{N_s}$, where P denotes the power of the transmitted signal. Let us assume that the training process is divided into S stages corresponding to the S stages of precoder and combiner design. Then, corresponding to the channel estimation, (1) at the s-th stage can be expressed to show explicitly

the vectorized beam-space channels as

$$\boldsymbol{y}_s = \sqrt{P}\Big(\boldsymbol{F}_s \otimes \boldsymbol{W}_s^H\Big)\big(\boldsymbol{A}_T^* \otimes \boldsymbol{A}_R\big)\boldsymbol{h}_b + \boldsymbol{e}_s,$$
$$s = 1, 2, \ldots, S \quad (19)$$

where $\boldsymbol{y}_s$ is the received measurement vector at Stage s, $\boldsymbol{e}_s = vec\{(\boldsymbol{W}^H \boldsymbol{n}_s\}$ is the corresponding noise vector, $\boldsymbol{F}_s$ and $\boldsymbol{W}_s$ are the precoder and combiner, respectively, applied at the s-th stage, which are designed based on the AoD/AoA identified at the $(s-1)$-th stage [17].

Based on (19), the OMP algorithm can then be employed to estimate the channels. Furthermore, from (19) we can know that when increasing the Stage s, the codebook's resolution becomes higher. Therefore, a higher resolution precoder or combiner can be obtained, but at lower complexity than the approaches that directly operate on the high resolution codebook, as discussed, for example, in [17].

However, due to the properties of the OMP algorithm, the above-described adaptive codebook-based channel estimation yields relatively good performance, only when the systems are operated in relatively high SNR region [17]. It is unable to achieve a desired performance at low and even moderate SNR. To this end, below we extend the method for the channel estimation in OFDM systems, which is capable of achieving desirable performance at low SNR.

B. PROPOSED ADAPTIVE CODEBOOK-BASED CHANNEL ESTIMATION WITH JOINT MULTI-CARRIER DECISION MAKING

In the OFDM-based MIMO systems, the channel matrix of the N_c subcarriers can be written as $\boldsymbol{H} = [\boldsymbol{H}^{(1)}, \boldsymbol{H}^{(2)}, \ldots, \boldsymbol{H}^{(N_c)}]$, where $\boldsymbol{H}^{(n)}$ is the channel matrix of the nth subcarrier, as shown in the form of (14). Then, when the above described adaptive codebook-based channel estimation is extended to the OFDM-MIMO scenario, corresponding to (19), the received signals from the N_c subcarriers at the s-th stage can be expressed as

$$\boldsymbol{y}_s = \Big(\big(\boldsymbol{I}_{N_c} \otimes \boldsymbol{F}_s\big) \otimes \boldsymbol{W}_s^H\Big)\boldsymbol{h} + \boldsymbol{e}_s,$$
$$s = 1, 2, \ldots, S \quad (20)$$

where $\boldsymbol{y}_s = [(\boldsymbol{y}_s^{(1)})^T, \ldots, (\boldsymbol{y}_s^{(N_c)})^T]^T$, $\boldsymbol{W}_s$ and $\boldsymbol{F}_s$ are the receiver combiner and transmitter precoder, respectively, $\boldsymbol{e}_s = [(\boldsymbol{e}_s^{(1)})^T, (\boldsymbol{e}_s^{(2)})^T, \ldots, (\boldsymbol{e}_s^{(N_c)})^T]^T$ is the vectorized noise, and $\boldsymbol{h} = vec(\boldsymbol{H})$, which, with the aid of (15), can be expressed as

$$\boldsymbol{h} = \big(\big(\boldsymbol{I}_{N_c} \otimes \boldsymbol{A}_T^*\big) \otimes \boldsymbol{A}_R\big)\boldsymbol{h}_b, \quad (21)$$

where $\boldsymbol{h}_b = [(\boldsymbol{h}_b^{(1)})^T, (\boldsymbol{h}_b^{(2)})^T, \ldots, (\boldsymbol{h}_b^{(N_c)})^T]^T \in \mathbb{C}^{G_t G_r N_c \times 1}$ with $\boldsymbol{h}_b^{(n_c)}$ as defined in (15).

Note that, when the subcarriers are individually considered, the received signals corresponding to a subcarrier can be represented as

$$\boldsymbol{y}_s^{(n_c)} = \Big(\boldsymbol{F}_s \otimes \boldsymbol{W}_s^H\Big)\boldsymbol{h}^{(n_c)} + \boldsymbol{e}_s^{(n_c)}$$
$$n_c = 1, 2, \ldots, N_c; \quad s = 1, 2, \ldots, S, \quad (22)$$
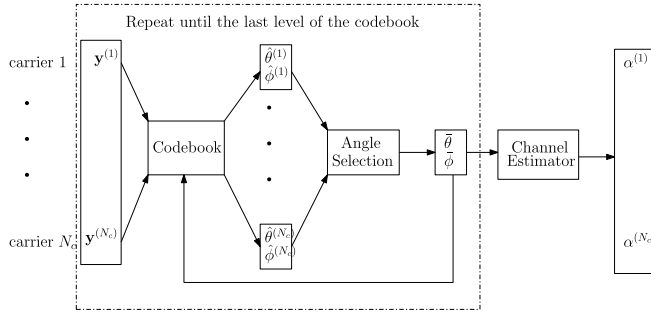
FIGURE 3. Block diagram of our proposed channel estimation technique.

with $\boldsymbol{h}^{(n_c)}$ defined by

$$\boldsymbol{h}^{(n_c)} = \left(\boldsymbol{A}_T^* \otimes \boldsymbol{A}_R\right)\boldsymbol{h}_b^{(n_c)}, \ \ n_c = 1, 2, \ldots, N_c. \tag{23}$$

From (22) it can be implied that the precoder $\boldsymbol{F}_s$ and combiner $\boldsymbol{W}_s$ are the same for all the subcarriers, as they are only depended on the AoDs/AoAs. Hence, their design can be enhanced by exploiting the AoDs/AoAs information extracted from all the N_c subcarriers. However, the conventional adaptive codebook-based design analyzed in Section III-A is carried out at the individual subcarrier level without taking the advantage of this relationship, making channel estimation have relatively low reliability in low to medium SNR regions. Hence, in our proposed approach, we will make use of this relationship to improve the performance of channel estimation, including the estimation of AoDs/AoAs and channel gains.

Specifically in our proposed approach, during a stage, the precoder (or combiner) is designed based on the estimated angle provided by the most of subcarriers. In this way, a more accurate codeword can be identified, based on which, hence, a better precoder (or combiner) can be designed for use at the next stage. Finally, after S stages of refinement, a better precoder (or combiner) of full resolution can be obtained, based on which more accurate estimate to the channel gain can be obtained.

The structure of our proposed channel estimation is demonstrated in Fig. 3. As shown in Fig. 3, at a stage, N_c estimates of $\hat{\theta}^{(n_c)}$ (or $\hat{\phi}^{(n_c)}$), $n_c \in \{1, 2, \ldots, N_c\}$, for the same target AoD/AoA are first obtained separately from the N_c subcarriers, where $\theta^{(n_c)}$ and $\phi^{(n_c)}$ are the estimated AoA/AoD angles from the n_c-th subcarrier. Then, an angle selection procedure is implemented to obtain the most accurate estimate of $\hat{\theta}^{(n_c)}$ (or $\hat{\phi}^{(n_c)}$). In our method, for the sake of simplicity, the majority vote based angle selection is used, which selects the $\hat{\theta}^{(n_c)}$ (or $\hat{\phi}^{(n_c)}$) occurred with the highest frequency among the N_c estimates as the final estimate of $\bar{\theta}$ (or $\bar{\phi}$) at the stage.[2] Then, based on the estimated angles $\bar{\theta}$ and $\bar{\phi}$, the precoder and combiner are designed for use at the next stage, until the final stage of S, which generates the precoder and combiner for the following channel

---

2. Note that, in the beamspace representation, the AoA/AoD are in discrete form.

Algorithm 1: Proposed Channel Estimation Algorithm

Data: Both transmitter and receiver know
$\quad\quad N = G_T = G_R, K, L_e$, codebook $\mathcal{F}$ and $\mathcal{W}$,
$\quad\quad$ angle grid $\boldsymbol{A}_F, \boldsymbol{A}_W$

Input: $S = \log_K N, \hat{\boldsymbol{H}} = 0$

1 $l = 1$
2 **if** $l \leq L_e$ **then**
3 $\quad \hat{\boldsymbol{h}} = vec\{\hat{\boldsymbol{H}}\}$
4 $\quad k_1^{(t)} = 1; k_1^{(r)} = 1; s = 1$
5 $\quad$ **if** $s \leq S$ **then**
6 $\quad\quad$ Transmitter applies $[\boldsymbol{F}_{(s,k_s^{(t)})}]$ for precoding on each carrier
7 $\quad\quad$ Receiver uses $[\boldsymbol{W}_{(s,k_s^{(r)})}]$ for combining on each carrier
8 $\quad\quad$ Received signals of N_c subcarriers:
9 $\quad\quad \boldsymbol{y} = \left(\boldsymbol{I}_{N_c} \otimes \boldsymbol{F}_{(s,k_s^{(t)})}\right) \otimes \boldsymbol{W}_{(s,k_s^{(t)})}^H (\boldsymbol{h} - \hat{\boldsymbol{h}}) + \boldsymbol{e}$
10 $\quad\quad i = 1$
11 $\quad\quad$ **if** $i \leq N_c$ **then**
12 $\quad\quad\quad \boldsymbol{y}^{(i)} = \boldsymbol{y}((i-1)K + 1 : i * K)$
13 $\quad\quad\quad \hat{m}(i) = \arg\max_{\forall m} \|\boldsymbol{y}^{(i)}(m)\|$
14 $\quad\quad\quad i = i + 1$
15 $\quad\quad$ **end**
16 $\quad\quad p = \text{Mode}(\hat{m})$
17 $\quad\quad \hat{m}_t = \lceil p/K \rceil$
18 $\quad\quad \hat{m}_r = p - (\hat{m}_t - 1)K$
19 $\quad\quad k_{s+1}^{(t)} = (\hat{m}_t - 1)K + m_t$
20 $\quad\quad k_{s+1}^{(r)} = (\hat{m}_r - 1)K + m_r$
21 $\quad\quad s = s + 1$
22 $\quad$ **end**
23 $\quad \hat{\boldsymbol{h}}_b = \frac{L_e}{\sqrt{N_t N_r}}[\boldsymbol{y}(p, :)]$
24 $\quad \hat{\boldsymbol{H}} = \hat{\boldsymbol{H}} + \frac{\sqrt{N_t N_r}}{L_e}\hat{\boldsymbol{h}}_b \otimes [\boldsymbol{A}_F(:, k_{s+1}^{(t)})\boldsymbol{A}_W^H(:, k_{s+1}^{(t)})]$
25 $\quad l = l + 1$
26 **end**

---

gain estimation and data transmission. For example, after the precoder $\boldsymbol{F}$ and combiner $\boldsymbol{W}$ have been obtained from the above-described procedure, $\hat{\boldsymbol{h}}_b^{(n_c)}$ of the n_c-th subcarrier can be estimated from the received signals $\boldsymbol{y}^{(n_c)}$ of (22) with $\boldsymbol{F}_s$ and $\boldsymbol{W}_s$ replaced by the finally designed precoder $\boldsymbol{F}$ and combiner $\boldsymbol{W}$.

It can be understood that owing to the selection procedure involved for the estimation of AoA/AoD, the proposed algorithm can reduce the influence of noise, especially in the low SNR scenario. Consequently, the estimation performance can be improved, which will be further illustrated by the simulation results in Section IV.

The details of the proposed channel estimation algorithm is summarized as Algorithm 1. In more detail, in Algorithm 1, the codebook $\mathcal{F}$ and $\mathcal{W}$ are chosen to match the angle grids of $\boldsymbol{A}_F$ and $\boldsymbol{A}_W$, respectively. L_e is the number of the dominant paths required to be resolved and estimated. As shown in the algorithm, the channels of the L_e paths are estimated
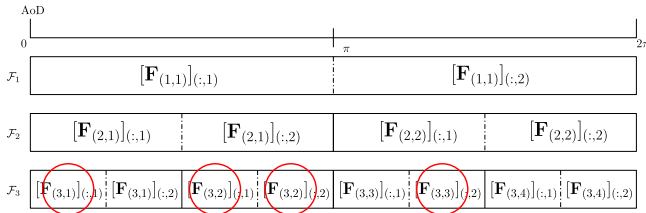
FIGURE 4. Example for illustrating the proposed channel estimation scheme.

by L_e iteration, each iteration estimates the channel parameters, including an AoD, an AoA and a gain, of one path of the N_c subcarriers. To estimate one path of the N_c subcarriers, S stages of refinements are carried out based on the codebooks at different stages, which are designed according to (18). After S stages, for each of the N_c subcarriers, the codeword yielding the largest correlation value with the received signal is identified. Then, the codewords, which correspond to AoDs/AoAs, produced from the N_c subcarriers are compared and the one presenting the most number of times is selected as the estimated codeword corresponding to a specific AoD/AoA. Then, based on the estimated codeword (or AoD/AoA), the precoder/combiner is formed, which is used for estimating the path gain as well as for the following data transmission. Then, as shown in Algorithm 1, the above-mentioned is repeated L_e times until the channel parameters of all the L_e paths are estimated. Note that, to estimate the parameters of the l-th, $l = 2, 3, \ldots, L_e$, paths, the paths having been estimated during the previous iterations are cancelled from the received signal, as shown on Line 9 in Algorithm 1, to remove their effect on the estimation of the rest paths.

Below we use an example supported by Fig. 4 to further explain our proposed method. Again, let us assume that $S = 3$ and $K = 2$. Hence, the codebooks, as shown in Fig. 4, have the same structures as that in Fig. 2. Let us assume that there are $L_e = 4$ target beams to be estimated, which fall respectively in the sub-ranges highlighted by the red circles in Fig. 4. The AoD and AoA of each of these beams need to be estimated before estimating the gain of the beam. In total, 4 iterations are required for estimating the parameters of the 4 beams.

Specifically, in the first iteration, the first stage codebook having one subset containing two codewords is applied by all the N_c subcarriers to respectively identify their desired codewords. The two codewords, namely, $[\boldsymbol{F}_{(1,1)}]_{(:,1)}$ and $[\boldsymbol{F}_{(1,1)}]_{(:,2)}$, are designed using (18) so that: a) they are orthogonal to each other, and b) one codeword matches to the beam(s) in the angle range of $[0, \pi)$ and the other one to the beam(s) in the angle range of $[\pi, 2\pi)$. In practice, it can be expected that the codewords identified from the N_c subcarriers may be different, due to the effect of noise and possibly other interference. However, for the example considered, we can expect that most of the estimated codewords by the N_c subcarriers would be $[\boldsymbol{F}_{(1,1)}]_{(:,1)}$, because 3 out of the 4 target beams fall in this range. Hence, we

assume that the joint multi-carrier assisted decision making process yields $[\boldsymbol{F}_{(1,1)}]_{(:,1)}$ as the estimate to the beam vector at Stage 1, based on which a precoder (similarly a combiner) can be designed for the next stage.

Since the first sub-region corresponding to $[\boldsymbol{F}_{(1,1)}]_{(:,1)}$ is identified at the first stage, during the second stage, the codewords $[\boldsymbol{F}_{(2,1)}]_{(:,1)}$ and $[\boldsymbol{F}_{(2,1)}]_{(:,2)}$ will be constructed, again, using (18). Then, these two codewords are used to identify a beam either in the sub-region corresponding to $[\boldsymbol{F}_{(2,1)}]_{(:,1)}$ or in the sub-region corresponding to $[\boldsymbol{F}_{(2,1)}]_{(:,2)}$. The processings are the same as that in stage 1. This time, let us assume that the beam vector estimated from most of the N_c subcarriers is $[\boldsymbol{F}_{(2,1)}]_{(:,2)}$, which is applied to design the precoder (or combiner) for use at the third stage.

Since $[\boldsymbol{F}_{(2,1)}]_{(:,2)}$ is estimated in the second stage, as shown in Fig. 4, the 2 codewords in stage 3 are $[\boldsymbol{F}_{(3,2)}]_{(:,1)}$, $[\boldsymbol{F}_{(3,2)}]_{(:,2)}$. Then, following the same procedure as that in stage 1 or 2, one of these two codeword is selected, which represents a beam vector estimated in the first iteration. Let us assume that beam vector estimated is $[\boldsymbol{F}_{(3,2)}]_{(:,1)}$.

Similarly, we assume that the receiver find a beam vector, which is assumed to be $[\boldsymbol{W}_{(3,2)}]_{(:,2)}$. The receiver uses a feedback channel to inform the transmitter $[\boldsymbol{F}_{(3,2)}]_{(:,1)}$. Then, the gain of the selected beam on the n_c-th subcarrier can be obtained as [17].

$$\alpha_1^{(n_c)} = \frac{\sqrt{\frac{L}{N_t N_r}} y_{max}^{(n_c)}}{[\boldsymbol{W}_{(3,2)}]_{(:,2)}^H \boldsymbol{A}_R * \boldsymbol{A}_T^H [\boldsymbol{F}_{(3,2)}]_{(:,1)}}, \quad n_c = 1, 2, \ldots, N_c \tag{24}$$

where $y_{max}^{(n_c)}$ denotes the maximum measurement output of the n_c-th subcarrier in this iteration.

To this point, the channel parameters of one beam, including AoD, AoA and gain, are obtained. Using this knowledge, the channel matrix accounting for the first beam can be formed as

$$\hat{\boldsymbol{H}}_1^{(n_c)} = \sqrt{\frac{N_t N_r}{L}} [\boldsymbol{W}_{(3,2)}]_{(:,2)}^H \boldsymbol{A}_R * \alpha_1^{(n_c)} * \boldsymbol{A}_T^H [\boldsymbol{F}_{(3,1)}]_{(:,1)}. \tag{25}$$

Afterwards, the beam vector $[\boldsymbol{F}_{(3,2)}]_{(:,1)}$ is cancelled from the measurement set of transmitter and the beam vector $[\boldsymbol{W}_{(3,2)}]_{(:,2)}$ is removed from the measurement set of receiver. Then, the algorithm enters the second iteration to identify another beam vector for precoder and also a beam vector for combiner. The above steps are repeated until all the $L_e = 4$ paths as well as their gains are estimated, meaning the completion of the estimation process.

In comparison with the traditional adaptive codebook based channel estimation, the proposed method can mitigate the effect noise, owing to the joint multi-carrier assisted decision making process involved for obtaining more reliable estimates at different stages. Benefiting from the more reliable estimates provided at different stages, the proposed method is capable of achieving better performance, especially in noisy scenarios, than the conventional codebook based channel estimation, as shown in the next section.
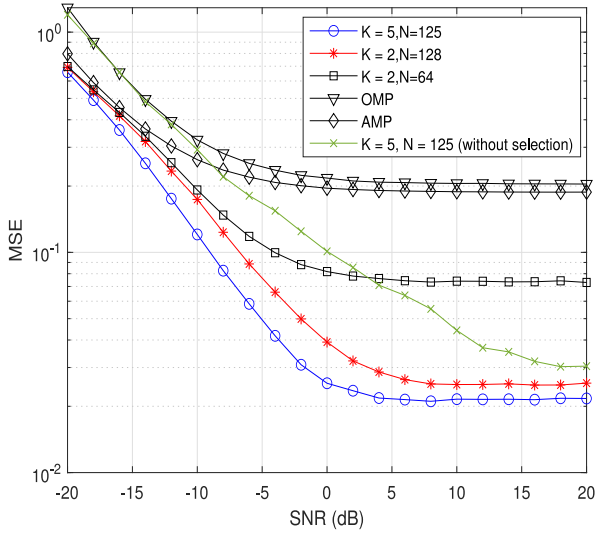
FIGURE 5. MSE performance of channel estimation with different *K* and *N* values.

IV. SIMULATION RESULTS AND DISCUSSION

In this section, we present the simulation results to compare the performance of the proposed channel estimation scheme and that of the conventional adaptive codebook-based channel estimation. In our simulations, the system model considered in Fig. 1 is assumed to have $N_c = 256$ subcarriers, $N_t = 32$ transmit antennas, $N_r = 16$ receive antennas, $N_{RF}^{(t)} = N_{RF}^{(r)} = 10$ RF chains, and the resolution is assumed as $N = G_T = G_R$. The channel model described in (4) has $L = 4$ paths. Both the Mean Square Error (MSE) and the achievable rate are considered. Specifically, the MSE is evaluated as

$$\text{MSE} = \mathbb{E}\left[\frac{\|\hat{\boldsymbol{H}} - \boldsymbol{H}\|^2}{N_t N_s N_c}\right], \qquad (26)$$

where $\|\cdot\|^2$ is the square of the 2-norm. Note that, since the channel has been normalized to have unity power, the MSE of (26) is in fact the normalized MSE. The achievable rate is evaluated by the formula [12]

$$R = \mathbb{E}\left[\log_2 \det\left(\boldsymbol{I}_{N_s} + \frac{1}{N_s}\boldsymbol{R}_n^{-1}\boldsymbol{W}^H\boldsymbol{H}\boldsymbol{F}\boldsymbol{F}^H\boldsymbol{H}^H\boldsymbol{W}\right)\right], \quad (27)$$

where the expectation is taken with respect to the mmWave channels, and $\boldsymbol{R}_n = \sigma^2 \boldsymbol{W}^H \boldsymbol{W}$ is the noise's covariance matrix after the combining processing [11], where $\boldsymbol{W} = \boldsymbol{W}_{RF}\boldsymbol{W}_{BB}$, while $\boldsymbol{F} = \boldsymbol{F}_{RF}\boldsymbol{F}_{BB}$. Note that in our studied schemes, the hybrid beamforming method employed is the same as that considered in [12].

Fig. 5 shows the MSE performance of the proposed channel estimation with respect to K, which is the number of subsets of codewords divided from one stage to the next, and N of the resolution in the last stage, i.e., S-th stage, of the codebook. As shown in Fig. 5, we compare the cases of $K = 5, N = 125$; $K = 2, N = 128$; and $K = 2, N = 64$. As the benchmark, the MSE performance of the conventional adaptive codebook-based channel estimation with $K = 5$ and

$N = 125$ is provided. Furthermore, the MSE performance of the traditional OMP algorithm [27] and of the Approximate Message Passing (AMP) algorithm [27], both of which assume $N = 125$, are compared. As shown in Fig. 5, the MSE achieved by the proposed algorithm is about 10 times lower than that achieved by conventional OMP and AMP based channel estimation algorithms. The reason behind is that during the training stage, in our codebook-based channel estimation, the precoder and combiner are designed from the codebook with the estimated AoA/AoD angles. By contrast, in the OMP and AMP based algorithms, the precoder and combiner are randomly selected, which hence results in the worse performance of channel estimation. The above observation also implies that, the target beam is most likely to align with the path having the maximum power, which is used to estimate the AoA/AoD angles and the channel gains in our algorithm. As shown in Fig. 5, for $K = 5$ and $N = 125$, the proposed channel estimation scheme also significantly outperforms the benchmarker of the conventional adaptive codebook-based channel estimation. Specifically at SNR= 0dB, the MSE yielded by the benchmark is about 8 times higher than that obtained by our proposed channel estimation. Considering only the proposed channel estimation scheme, as shown in Fig. 5, an increased resolution N of the beamspace provides more accurate channel estimation. Furthermore, for a similar resolution N of equating 125 and 128, the value of K affects positively the MSE performance, and a larger value of K yields a lower MSE of the channel estimation. However, in the cases that the resolutions of N are similar, when K increases, the complexity of each stage is higher, since there are more elements in the received signal to be compared. On the other side, when the value of K is small, there will be more stages in the codebook, which needs more times of codebook design and training, as well as more resources for feeding back the designed precoder to transmitter. Therefore, in practice, an appropriate value of K should be chosen to attain a good balance among the above-mentioned issues.

Fig. 6 shows the MSE performance of the sparse Bayesian learning (SBL) channel estimation [28], conventional adaptive codebook-based channel estimation and the adaptive codebook-based channel estimation, when a resolution of $N = 25$ is assumed. In this study, we consider a relatively low resolution case, because the SBL channel estimation can achieve very good estimation performance at relatively low resolution, by demanding a significantly increased computational complexity.[3] As shown in Fig. 6, the proposed method achieves better performance than the conventional adaptive codebook-based channel estimation before the two MSE curves converge at about 27dB. The MSE achieved by the proposed method is about half of that attained by the SBL algorithm, when the SNR is less than about 13dB. When

---

3. Please note that a low resolution is used for simulating the SBL algorithm in Fig. 6, due to the high computational complexity required for simulating the SBL algorithm with the resolutions used in Fig. 5.
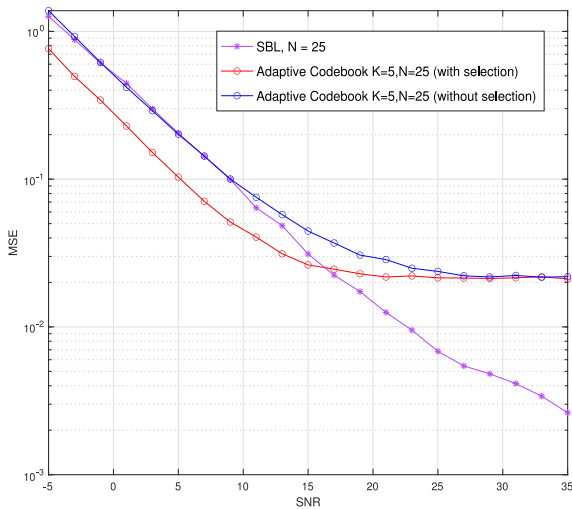
FIGURE 6. Comparison of MSE performance of the codebook-based and SBL-based channel estimation, when $N_t = 8$ and $N_r = 8$.
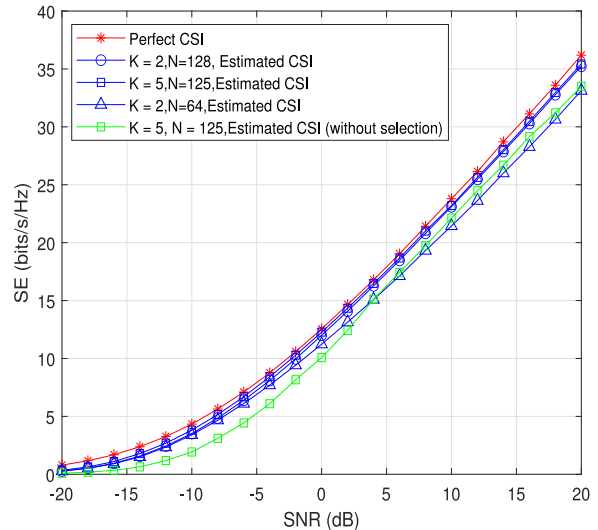

FIGURE 7. Achievable rates of the OFDM systems with respectively the proposed channel estimation and the conventional codebook-based channel estimation.

the SNR is higher than about 17 dB, the SBL algorithm shows better MSE performance than the proposed adaptive codebook-based algorithm. However, we should note again that the computational complexity of the SBL algorithm is much higher than that of the adaptive codebook-based algorithms [29]. For example, for a system employing 8 transmit antennas and 8 receive antennas, the number of multiplications required by the SBL algorithm is around 10^8. On the other hand, there are less than 10^2 multiplications required by the adaptive codebook-based channel estimation algorithms. Therefore, when considering the performance versus complexity trade-off, the proposed channel estimator constitutes a highly promising candidate, especially, in the applications where a low-complexity channel estimator for operation in low SNR region is desired.

Fig. 7 depicts the spectral efficiency (SE) performance of the OFDM systems employing the proposed channel estimation or the conventional adaptive codebook-based channel estimation, when different values of K and N are considered. In the considered OFDM systems, the hybrid beamformers and combiners are designed based on the estimated channels. As shown in Fig. 7, for the proposed channel estimation, as the resolution N increases, the achievable rates of the OFDM systems relying on the estimated CSI are close to that achieved by assuming perfect CSI. The proposed channel estimation in all the considered cases performs better than the conventional counterpart in the low SNR region. By contrast, when SNR is higher than about 4dB, the conventional one achieves higher SE than the proposed one when $K = 2$ and $N = 64$, but it is still outperformed by the proposed channel estimation, when $K = 2$ and $N = 128$ or $K = 5$ and $N = 125$.

V. CONCLUSION

In this paper, we have proposed an improved adaptive codebook-based channel estimation algorithm for operation in the mmWave OFDM systems. With the aid of the channels estimated from multiple subcarriers for joint decision making, the algorithm is capable of providing more accurate AOD/AOA estimations at the different estimation stages. Consequently, the transmitter beamformer and receiver combiner can be designed on the basis of the more accurate CSI, which ultimately enhances the performance of the mmWave OFDM systems. Our simulation results demonstrate that the proposed algorithm performs much better than the existing benchmark algorithm, i.e., the adaptive codebook channel estimation algorithm, especially in the low SNR region. Hence, it is capable of achieving the desirable channel estimation performance, while enjoying the low complexity merit of the adaptive codebook-based channel estimation algorithm. There are various methods that may be introduced to further improve the performance-complexity trade-off of our codebook-based channel estimation for mmWave OFDM systems. Our future research on the topic will be considering the deep learning methods for the codebook design, beam search, and the design of precoder and combiner.

REFERENCES

[1] I. A. Hemadeh, K. Satyanarayana, M. El-Hajjar, and L. Hanzo, "Millimeter-wave communications: Physical channel models, design considerations, antenna constructions, and link-budget," *IEEE Commun. Surveys Tuts.*, vol. 20, no. 2, pp. 870–913, 2nd Quart., 2018.

[2] X. Wang *et al.*, "Millimeter wave communication: A comprehensive survey," *IEEE Commun. Surveys Tuts.*, vol. 20, no. 3, pp. 1616–1653, 3rd Quart., 2018.

[3] T. S. Rappaport *et al.*, "Millimeter wave mobile communications for 5G cellular: It will work!" *IEEE Access*, vol. 1, pp. 335–349, 2013.

[4] R. W. Heath, N. González-Prelcic, S. Rangan, W. Roh, and A. M. Sayeed, "An overview of signal processing techniques for millimeter wave MIMO systems," *IEEE J. Sel. Topics Signal Process.*, vol. 10, no. 3, pp. 436–453, Apr. 2016.

[5] I. Ahmed *et al.*, "A survey on hybrid beamforming techniques in 5G: Architecture and system model perspectives," *IEEE Commun. Surveys Tuts.*, vol. 20, no. 4, pp. 3060–3097, 4th Quart., 2018.

[6] E. G. Larsson, O. Edfors, F. Tufvesson, and T. L. Marzetta, "Massive MIMO for next generation wireless systems," *IEEE Commun. Mag.*, vol. 52, no. 2, pp. 186–195, Feb. 2014.

[7] L. Lu, G. Y. Li, A. L. Swindlehurst, A. Ashikhmin, and R. Zhang, "An overview of massive MIMO: Benefits and challenges," *IEEE J. Sel. Topics Signal Process.*, vol. 8, no. 5, pp. 742–758, Oct. 2014.

[8] F. Rusek *et al.*, "Scaling up MIMO: Opportunities and challenges with very large arrays," *IEEE Signal Process. Mag.*, vol. 30, no. 1, pp. 40–60, Jan. 2013.

[9] Z. Pi and F. Khan, "An introduction to millimeter-wave mobile broadband systems," *IEEE Commun. Mag.*, vol. 49, no. 6, pp. 101–107, Jun. 2011.

[10] K. Satyanarayana, M. El-Hajjar, P.-H. Kuo, A. Mourad, and L. Hanzo, "Hybrid beamforming design for full-duplex millimeter wave communication," *IEEE Trans. Veh. Technol*, vol. 68, no. 2, pp. 1394–1404, Feb. 2019.

[11] A. Alkhateeb, O. El Ayach, G. Leus, and R. W. Heath, "Hybrid precoding for millimeter wave cellular systems with partial channel knowledge," in *Proc. Inf. Theory Appl. Workshop (ITA)*, 2013, pp. 1–5.

[12] O. El Ayach, S. Rajagopal, S. Abu-Surra, Z. Pi, and R. W. Heath, "Spatially sparse precoding in millimeter wave mimo systems," *IEEE Trans. Wireless Commun.*, vol. 13, no. 3, pp. 1499–1513, Mar. 2014.

[13] A. Liao, Z. Gao, H. Wang, S. Chen, M.-S. Alouini, and H. Yin, "Closed-loop sparse channel estimation for wideband millimeter-wave full-dimensional MIMO systems," *IEEE Trans. Commun.*, vol. 67, no. 12, pp. 8329–8345, Dec. 2019.

[14] J. Rodríguez-Fernández, N. González-Prelcic, K. Venugopal, and R. W. Heath, "Frequency-domain compressive channel estimation for frequency-selective hybrid millimeter wave MIMO systems," *IEEE Trans. Wireless Commun.*, vol. 17, no. 5, pp. 2946–2960, May 2018.

[15] Z. Gao, L. Dai, S. Han, I. Chih-Lin, Z. Wang, and L. Hanzo, "Compressive sensing techniques for next-generation wireless communications," *IEEE Wireless Commun.*, vol. 25, no. 3, pp. 144–153, Jun. 2018.

[16] S. A. Busari, K. M. S. Huq, S. Mumtaz, L. Dai, and J. Rodriguez, "Millimeter-wave massive MIMO communication for future wireless systems: A survey," *IEEE Commun. Surveys Tuts.*, vol. 20, no. 2, pp. 836–869, 2nd Quat., 2018.

[17] A. Alkhateeb, O. El Ayach, G. Leus, and R. W. Heath, "Channel estimation and hybrid precoding for millimeter wave cellular systems," *IEEE J. Sel. Topics Signal Process.*, vol. 8, no. 5, pp. 831–846, Oct. 2014.

[18] F. Talaei and X. Dong, "Hybrid mmWave MIMO-OFDM channel estimation based on the multi-band sparse structure of channel," *IEEE Trans. Commun.*, vol. 67, no. 2, pp. 1018–1030, Feb. 2019.

[19] X. Gao, L. Dai, S. Han, I. Chih-Lin, and X. Wang, "Reliable beamspace channel estimation for millimeter-wave massive MIMO systems with lens antenna array," *IEEE Trans. Wireless Commun.*, vol. 16, no. 9, pp. 6010–6021, Sep. 2017.

[20] J. Tan and L. Dai, "Wideband channel estimation for THz massive MIMO," *China Commun.*, vol. 18, no. 5, pp. 66–80, May 2021.

[21] J. A. Tropp and A. C. Gilbert, "Signal recovery from random measurements via orthogonal matching pursuit," *IEEE Trans. Inf. Theory*, vol. 53, no. 12, pp. 4655–4666, Dec. 2007.

[22] J. Lee, G.-T. Gil, and Y. H. Lee, "Channel estimation via orthogonal matching pursuit for hybrid MIMO systems in millimeter wave communications," *IEEE Trans. Commun.*, vol. 64, no. 6, pp. 2370–2386, Jun. 2016.

[23] C. Hu, L. Dai, T. Mir, Z. Gao, and J. Fang, "Super-resolution channel estimation for mmWave massive MIMO with hybrid precoding," *IEEE Trans. Veh. Technol.*, vol. 67, no. 9, pp. 8954–8958, Sep. 2018.

[24] L.-L. Yang, *Multicarrier Communications*. Chichester, U.K.: Wiley, 2009.

[25] H. Liu, S. Lu, M. El-Hajjar, and L.-L. Yang, "Machine learning assisted adaptive index modulation for mmWave communications," *IEEE Open J. Commun. Soc.*, vol. 1, pp. 1425–1441, 2020.

[26] D. J. Love, R. W. Heath, V. K. N. Lau, D. Gesbert, B. D. Rao, and M. Andrews, "An overview of limited feedback in wireless communication systems," *IEEE J. Sel. Areas Commun.*, vol. 26, no. 8, pp. 1341–1365, Oct. 2008.

[27] X. Wei, C. Hu, and L. Dai, "Deep learning for beamspace channel estimation in millimeter-wave massive MIMO systems," *IEEE Trans. Commun.*, vol. 69, no. 1, pp. 182–193, Jan. 2021.

[28] D. P. Wipf and B. D. Rao, "Sparse Bayesian learning for basis selection," *IEEE Trans. Signal Process.*, vol. 52, no. 8, pp. 2153–2164, Aug. 2004.

[29] K. Liu, X. Li, J. Fang, and H. Li, "Bayesian mmWave channel estimation via exploiting joint sparse and low-rank structures," *IEEE Access*, vol. 7, pp. 48961–48970, 2019.